Translational diffusion in a smectic-A phase by electron spin resonance imaging: The free-volume model

Jozef K. Moscicki,[a] Yeon-K. Shin,[b] and Jack H. Freed

Cornell University Baker Laboratory of Chemistry, Ithaca, New York 14853

The method of dynamic imaging of diffusion (DID)-ESR (electron spin resonance) has been utilized to study the anisotropy of translational diffusion of spin probes in the smectic A phase of a eutectic liquid crystal, S2. In particular, the nearly spherical perdeuterated-TEMPONE (PDT) and the rigid and elongated cholestane spin label (CSL) molecules were studied. Whereas $D_\perp$ (the coefficient of diffusion perpendicular to the nematic director) showed simple Arrhenius dependence for both probes, diffusion parallel to the director displayed two different temperature regimes with a changeover of $D_\parallel$ at $t^* \approx 26$–$27\,°C$. The regime above (below) t^* is characterized by weak (strong) translational ordering. For CSL the ratio $D_\perp / D_\parallel < 1$ above t^* which indicates nematiclike behavior, but below t^* the behavior is more smecticlike, i.e., $D_\perp / D_\parallel > 1$; for PDT $D_\perp / D_\parallel > 1$ over the whole temperature range. A free volume model is developed to interpret the activation energies associated with $D_\perp$ and $D_\parallel$ (i.e., $E_\perp$ and $E_\parallel$) in terms of the orientational and translational order parameters for the smectic phase and those for the spin probes. Also included are the variation of the compressibility across the smectic layer and the length of the probe relative to that of the thickness of the smectic layer. The fact that above t^* $E_\parallel / E_\perp$ is unity for CSL but a little greater that unity for PDT is interpreted as due to the weaker coupling of the larger CSL molecule to the weak translational ordering and compressibility variation. Below t^*, $E_\parallel / E_\perp$ becomes 1.52 and 1.80 for CSL and PDT, respectively, which may be interpreted in terms of enhancement of these smectic features. The free volume model may be used to analyze $E_\parallel$ and $E_\perp$ for self-diffusion and for a wide range of spin probes, including such very small probes like methane, as a function of the key parameters.

I. INTRODUCTION

Studies of translational diffusion were pioneered by Svedberg at the beginning of this century.[1,2] His many studies included the mass transport of an impurity (*m*-nitrophenol) in the ordered nematic phase of a mixture of *p*-azoxyanisole and *p*-azoxyphenetol, for two principal orientations of the nematic phase, i.e., parallel (∥) and perpendicular (⊥) to the nematic director. The amount of the impurity which had diffused was determined by chemical means. His major finding was that diffusion of nitrophenol in the nematic phase is anisotropic, the ratio of diffusion coefficients for both geometries being $D_\parallel / D_\perp = 1.41$.[1]

These studies were not followed up until the late sixties, when there was a rapid development of many techniques for measuring translational diffusion.[3–13] These techniques divide into two distinct categories. On the one hand, there are macroscopic (*macro*) methods which involve measurements of diffusion over distances several orders of magnitude larger than molecular dimensions, and are derived from the original idea of Svedberg of monitoring translational diffusion of impurities into the well prepared sample. These include radiotracers,[3] optically active

molecules,[4] charge carriers,[5,6] NMR with pulsed gradients,[7] and spin probes.[8,9] On the other hand, there are microscopic (*micro*) methods which are based on monitoring translational diffusion of molecules over distances of the order of molecular lengths. Typical examples are quasielastic (QNS)[10] or inelastic (INS)[11] neutron scattering, the frequency and temperature dependence of T_1, T_{ID}, and $T_{1\rho}$ in NMR,[12] and ESR (electron spin resonance) measurements of Heisenberg spin exchange (HE) between colliding radical pairs.[9,13]

The most extensive review of data on translational diffusion in liquid crystals was by Krüger more than 10 years ago.[14] A principal techniques for measuring diffusion in liquid crystals has been and remains NMR with pulsed gradients. Although results on smectic phases were sparse, only a few more recent studies have appeared,[15–18] since Krüger's review. In summary, the following is currently known about translational diffusion in the smectic phase. In most S_A systems, $D_\parallel < D_\perp$, although in systems which exhibit a significant nematic range, one may either observe $D_\parallel > D_\perp$,[18] or inversion from $D_\parallel > D_\perp$ typical for nematics to $D_\parallel < D_\perp$ on decreasing the temperature.[14,15,19] For the smectic A phase a better parameter to characterize the anisotropy of diffusion may well be the anisotropy of the activation energy. It appears that $E_\parallel$ is always greater than $E_\perp$. However, the ratio $E_\parallel / E_\perp$ is usually much larger for tracers than for self-diffusion.[14,15] In one instance, diffusion

[a] On leave from: Institute of Physics, Jagiellonian University, 30-059 Krakow, Poland.
[b] Present address: Jules Stein Eye Institute, UCLA School of Medicine, Los Angeles, CA 90024.

of methane in 40.6, a negative activation energy was observed.[15]

In recent years we have explored in our laboratory two approaches for studying translational diffusion of probes by ESR methods: HE between colliding spin probes[13] and dynamic imaging of diffusion (DID) of spin probes. The DID employed either standard CW-ESR imaging methods[8] or spectral-spatial ESR imaging.[9] HE provides an average relative microscopic diffusion coefficient, while DID can provide the macroscopic diffusion tensor. DID has proved to be a very reliable technique, and it is applicable to a range of problems, from the anisotropy of diffusion in liquid crystals,[20–22] to transverse (or lateral) diffusion in lyotropic liquid crystalline model membranes.[23,24] The introduction of spectral-spatial ESR imaging of diffusion in model membranes combines both the HE and DID-ESR methods to simultaneously measure *micro* (spectral) and *macro* (spatial) diffusion in the same system.[9] The recent development of Fourier-transform and two-dimensional Fourier-transform ESR imaging methods, may in the future greatly enhance the accuracy of such studies.[25]

The present paper reports on the first application of DID-ESR to the study of translational diffusion in the smectic phase. This study is partially motivated by our past work on molecular dynamics in liquid crystals by ESR techniques.[13,26–34] Most of the past work concentrated on rotational diffusion of spin probes in nematic and smectic phases. However, molecular dynamics at phase transitions has more recently received attention.[13,28,32–34] Theoretical[32] and experimental[33] studies of the linewidth divergence at the N–I and N–S_A phase transitions have shown a significant coupling of the orientational dynamics of spin probes to the critical fluctuations in the nematic and smectic order parameters, respectively. At both transitions translational diffusion can play a significant role in these phenomena. This is especially true for the N–S_A phase transition necessitating a better understanding of translational mobility of spin probes in the smectic phase. This need was also evidenced by our two-dimensional electron–electron double resonance (2D-ELDOR) study of spin probe dynamics in smectics,[29] which was successfully analyzed in terms of a model of rototranslational diffusion.[35]

We decided to study S2, an eutectic mixture of three cyanobiphenyls [4-cyano-4'-*n*-octyl biphenyl (8CB, 50%), 4-cyano-4'-*n*-decyl biphenyl (10CB, 39%), and 4-cyano-4'-*n*-decyloxy biphenyl (10OCB, 11%)] for three reasons. First it was utilized in our 2D-ELDOR study. Second, estimates of the microscopic translational diffusion coefficient are available for comparison.[11,29] Third, S2 exhibits a smectic phase over a wide temperature range (−1 to 48 °C) near room temperature.

Two different spin probes were selected for the study, the globular shaped PD-Tempone (PDT) and a rigid cigarlike cholestane molecule, CSL(3-doxyl derivative of cholestan-3-one). This choice offers two limiting cases of coupling between the smectic structure and the tracer. As our earlier studies have shown, the former spin probe is expelled from the higher density regions formed by the orientationally ordered aromatic cores of the liquid crystal

molecules toward less ordered aliphatic regions.[27,30] On the other hand, the rodlike and elongated CSL probe is expected to be more easily included in the hard-core regions. It is, therefore, of interest to learn about the molecular dynamics of both tracers along and across the smectic layers, and this is the second main goal of the present work.

In Sec. II we give a short outline of the theory of the DID-ESR experiment, as well as a description of the experimental procedure. The experimental results are presented in Sec. III and discussed in the light of existing theoretical models in Sec. IV. These results stimulated us to develop a theoretical approach to diffusion in the smectic phase, based on the free-volume model we explored for diffusional studies of CSL spin probe in model membranes;[24] the theory is outlined in Appendix A, and discussed in Sec. IV.

II. EXPERIMENT

A. Principles of DID-ESR

The basic concept of DID-CW-ESR is to monitor the time evolution of a nonuniform concentration of probes (spin probes) in one dimension. The time evolution of the concentration profile results from the translational diffusion of spin probes in a sample in which they are (initially) inhomogeneously distributed, as they tend to a (final) homogeneous state. A diffusion coefficient can then be determined from changes of the spin-probe distribution in time. The spin probe can be used as a marker for imaging the diffusion only if the shape of the ESR signal is independent of the concentration. It is, therefore, very important that at any time during the experiment, the concentration of spin probes at any point in a sample be low enough that the line broadening from HE can be neglected. It is also desirable that the concentration of spin probes is low enough for the translational diffusion to obey Fick's second law[36]

$$\frac{\partial C(x,t)}{\partial t} = D \frac{\partial^2 C(x,t)}{\partial x^2},\qquad(1)$$

where D is the (concentration-independent) diffusion constant.

DID-ESR takes advantage of the fact that the concentration profile is a convolution of the initial distribution with a Gaussian (broadening) function.[8] Following the convolution theorem,[37] the diffusion equation for one dimension in inverse wavelength space (k space) is given by[8]

$$\ln \mathscr{C}(k,t) = -4\pi^2 Dt \cdot k^2 + \ln \mathscr{C}_0(k),\qquad(2)$$

where $\mathscr{C}_0(k)$ and $\mathscr{C}(k,t)$ are FT distribution functions at the beginning of the experiment ($t=0$), and at time t, respectively.

The DID-ESR experiment simply monitors the component of diffusion in the direction of the magnetic field gradient, even though the sample is three dimensional. The ESR spectrum in the presence of a uniform magnetic field gradient is the convolution of the spectrum in the absence of gradient with the concentration profile. Thus again utilizing the convolution theorem,[37] one obtains in k space[8]

$$\mathcal{F}_g(k,t) = \mathcal{C}(k,t)\mathcal{F}_0(k), \qquad (3)$$

where $\mathcal{F}_0(k)$ and $\mathcal{F}_g(k,t)$ are the FT gradient-off and gradient-on ESR spectra.

Given spectra at two different times, t_i and t_j, Eq. (2) and Eq. (3) yield

$$\ln\frac{|\mathcal{F}_g(k,t_i)|}{|\mathcal{F}_g(k,t_j)|} = -4\pi^2 Dk^2 \Delta t_{ij}, \qquad (4)$$

where $\Delta t_{ij} = t_i - t_j$.

Although the principles of DID-ESR are simple, the experimental noise is a crucial constraint limiting the range of useful k modes that provide accurate data on the diffusion coefficient.[8] The lower limit of useful k modes, k_{MIN}, is at the point where the difference in the magnitude of the two paired spectra starts to overcome the experimental noise. On the other hand, the amplitude of the Fourier transformed ESR spectrum does decrease with increase of k, so it will reach the noise level at sufficiently high k, and this determines the upper bound of useful k modes, k_{MAX}. A basic requirement for a successful measurement is, of course, $k_{MIN} < k_{MAX}$.

A more rigorous discussion and estimation of optimum experimental conditions shows that both k_{MIN} and k_{MAX} depend on the signal-to-noise ratio, Δt_{ij}, the rms width of the concentration profile at the beginning of experiment, σ_i, and the ratio between the rms width of a "Gaussian" ESR line in the absence of a field gradient, Δ_B, and the magnetic field gradient $\nabla_x B$.

The useful range of k modes is monitored by analyzing the data in two steps.[8] First, the diffusion coefficient for each time pair is calculated from $\ln|I_g(k,t_i)/I_g(k,t_j)|$ vs $k^2\Delta t_{ij}$ [cf. Eq. (4)] for arbitrary k_{max}, (i.e., the k modes less than k_{max} are taken into account). Then, the first step is repeated for a range of values for k_{max}, and $D(k_{max})$ is obtained by averaging the values from all time pairs for each k_{max}. $D(k_{max})$ exhibits a plateau over a limited range of k modes (for which $k_{MIN} \leqslant k_{max} \leqslant k_{MAX}$), and the plateau region corresponds to the minimum rms error in the calculated diffusion coefficient, (cf. Figs. 4 and 5 of Ref. 8). Therefore, the D value at the plateau region is a reliable value of the diffusion coefficient.

B. DID-ESR instrumentation

The DID-ESR experiments were carried out at X band in a Varian model E12 spectrometer, with a TE_{102} narrow flange microwave cavity for $D_\perp$ measurements, and with a TM_{110} cylindrical cavity for $D_\parallel$ measurements. The standard first derivative mode with 100 kHz modulation and microwave powers of about 5 mW was used for recording spectra. The modulation amplitude was kept the same for the gradient-*on* and gradient-*off* spectra. A typical signal-to-noise ratio during DID-ESR was approximately 50; the sweep range was 100 G, and the sweep time was 60 s.

A pair of George Associates Lewis Coils, model 502 were employed to generate a linear magnetic field gradient across the cavity. Each of the Lewis Coils consists of a figure-eight coil. By appropriate connections between the electric terminals of each half of figure-eight coils, the coils

provided uniform field gradients either parallel or perpendicular to the main static field, with gradient uniformity better than 0.2% over 1.0 cm in the center of the cavity. The magnitude of the field gradient was continuously changed by varying the current through the coils.

The Lewis Coils were driven by a Sorensen DC Power Supply either model DCR150-10A or SRL20-25. Typically, when connected for the parallel field gradient, the Lewis Coils produced a gradient of 200 G/cm at a current of about 10 A. For the perpendicular arrangement, the gradient was 100 G/cm at a current of about 15 A.

Data from the Varian E12 were collected on a Leading Edge model D PC interfaced to an HP 3457 multimeter, which monitored the analog signal going to the XY recorder of the ESR spectrometer. All spectra were digitized to 1024 points.

To image along either direction, standard sample mounts and temperature controlling Dewars for each cavity were used. Temperature dependent studies were always performed by increasing the temperature. Each sample was used for three to five temperatures, chosen so as to cover much of the temperature range of interest. The temperature settings were different from sample to sample so as to ensure uniform coverage of the whole temperature range, and good statistics.

The progress of diffusion was monitored in the usual manner.[8] For each temperature, a series of ten consecutive gradient-*on* spectra, $I_g(B,t)$, were collected effectively every 100 s. Then, the concentration profile was allowed to develop over a period of $t_D = 2000$ to 4000 s and the series of ten measurements was repeated again. Both series were used for producing ten sets of time pairs to determine D, in the manner described in detail in Ref. 8.

C. Sample preparation

The liquid crystal S2 is an eutectic mixture shown in Fig. 1. It has transition temperatures, 320 (NI), 319 (SN), and 272 K (KS). It was purchased from BDH Chemicals and used without further purification. The two nitroxide free radicals PDT and CSL were obtained from MSD Isotopes and Syvar, respectively. Their full names as well as their chemical structure are shown in Fig. 1.

To obtain a quasi-one-dimensional sample, special sample holders were used. The sample holder consisted of two capillary sections joined by a piece of polyethylene tubing, see Fig. 2. A borosilicate glass capillary with an i.d. of about 1.1 mm (100 μl FISHERbrand Disposable micropipete) was cut in small sections, with special care to obtain perfectly cut edges perpendicular to the capillary axis. Some of the sections were later sealed on one end, cf. Fig. 2, to form the end of the holder (A). The capillary o.d. was matched with the i.d. of polyethylene tubing (Clay Adams's Intramedic, i.d. 1.57 mm) for a perfect joint seal (B). The length of section (A) was usually about 7 to 15 mm, the polyethylene joint a few mm, and the length of section (C) varied depending on the geometry of the experiment; for $D_\parallel$ measurements (TM cavity) the holder length was limited by the larger dimension of the
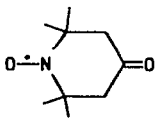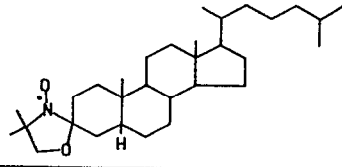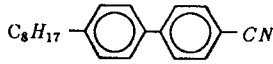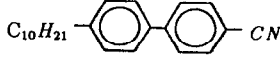
Acronym	Name	Structure
PD-Tempone	2,2',6,6'-tetramethyl-4-piperidine N-oxide (perdeuterated)	
CSL	(3',3'-dimethyloxazolidinyl-N-oxy 2',3-5α-cholestane	
S2	*Eutectic mixture of:* 50% 4-cyano 4'-n-octylbiphenyl (8CB) 39% 4-cyano 4'-n-decylbiphenyl (10CB) 11% 4-cyano 4'-n-decyloxybiphenyl (10OCB)	C_8H_{17} — CN $C_{10}H_{21}$ — CN $C_{10}H_{21}$ — O — CN
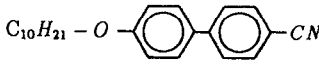
FIG. 1. Structures of spin probes and eutectic mixture S2.

sample hole of the TM cavity, about 15 mm; for the $D_\perp$ section (C) served as a support arm.

All samples were prepared in the same manner. First, a stock solution of spin probe in S2 was prepared. Typical concentrations for PDT and CSL were 2.5 and 3.5 mM, respectively. At these concentrations there was no evidence of HE. (A DSC study of the stock solutions showed just the expected phase transition temperatures for the isotropic–nematic, nematic–smectic, and smectic–crystalline transitions.) Then, samples with initial inhomo-

geneous distributions of spin probes were prepared in the following five steps:

(i) The end-sealed section of the capillary was filled with the pure liquid crystal nearly to the rim with the aid of a syringe, leaving a small space between the liquid surface and the capillary rim, ca 0.5 to 1.0 mm.

(ii) This space was filled with a small amount of the spin labeled material. Any excess material above the ridge was wiped away with the aid of a razor edge.

(iii) A small section of polyethylene tubing was pulled onto the open end of the capillary, and more pure material was added above the labeled material. The second layer of pure material usually filled about 3 to 4 mm of the polyethylene tubing.

(iv) Another open-ended section (C) of capillary was inserted into the tubing and pushed towards (A) to form a firm joint of capillary section rims, cf. Fig. 2.

(v) To obtain the ordered smectic phase, the sample was heated, immediately after preparation, to a temperature a few degrees above the clearing point and was placed in a strong magnetic field (above 0.8 T) for either parallel or perpendicular orientation. Subsequently it was slowly cooled down to ambient temperature. The quality of alignment was checked optically, and we found that one thermal cycle was sufficient to produce a good quality alignment.

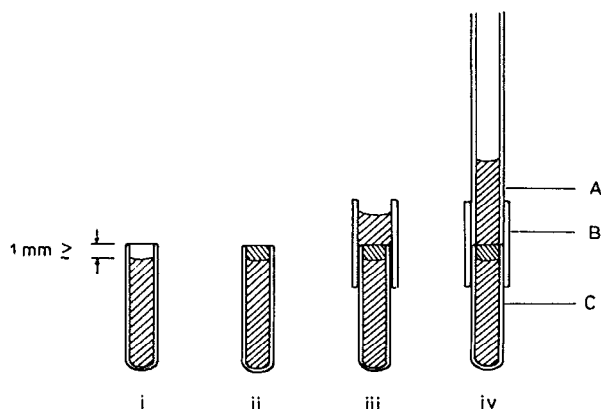The sample was then transferred to the spectrometer and the experimental run initiated.

FIG. 2. Schematic details of the sample preparation. The sample holder consisted of (A) and (C) capillary sections joined by (B) a piece of polyethylene tubing. (i) through (iv) correspond to consecutive steps in the sample preparation as described in text.
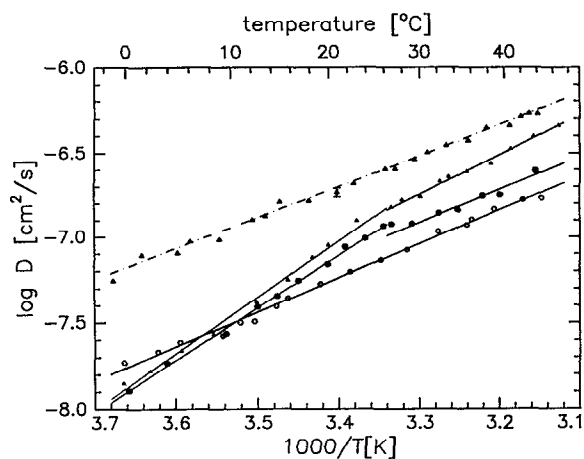
FIG. 3. Temperature dependence of diffusion constants of ($\bigcirc$,$\bullet$) CSL and ($\triangle$,$\blacktriangle$) PD-Tempone in the smectic phase of S2 liquid crystal, for the two principal geometries of the experiment, i.e., (open symbols) perpendicular and (full symbols) parallel to the director. The error bar corresponds to the standard deviation typical for all experimental points.

FIG. 4. Temperature dependence of $D_\perp/D_\parallel$ (top) for PDT and CSL and of $D_{\text{PDT}}/D_{\text{CSL}}$ (bottom) for longitudinal ($\parallel$) and translational ($\perp$) diffusion calculated from data in Fig. 3. The error bars correspond to a typical standard deviation resulting from the spline smoothing.

III. RESULTS

A summary of the studies of diffusion vs. temperature for both spin probes and for both principal geometries is given in Fig. 3 and Table I.

For diffusion perpendicular to the director axis, i.e., parallel to the smectic layers, the diffusion coefficients for both spin probes show typical Arrhenius dependence on temperature across the whole temperature range studied, i.e., $D(T) = D_0 \exp(-E_a/RT)$ (cf. Fig. 3). Both are characterized by a similar activation energy and prexponential factor (cf. Table I), although the value of the diffusion coefficient for the small PDT is nearly four times greater than that of the cigarlike CSL, cf. Fig. 4.

For diffusion perpendicular to the smectic layers (parallel to the director) two different temperature regimes are present. In each regime the log D vs. $1/T$ plots show Arrhenius behavior, but with different values of E_a and D_0, (cf. Fig. 3 and Table I). At high temperatures the activation energies are comparable to those for $D_\perp$, but at low temperatures they become more than 1.5 times greater. The ratios of activation energies, $E_\parallel/E_\perp$, for PDT and CSL are, respectively, 1.28 and 0.98 at high temperatures, and 1.80 and 1.52 at low temperatures. Interestingly, the values and the temperature dependence of $D_\parallel$ converge at low temperatures for both probes, cf. Figs. 3.
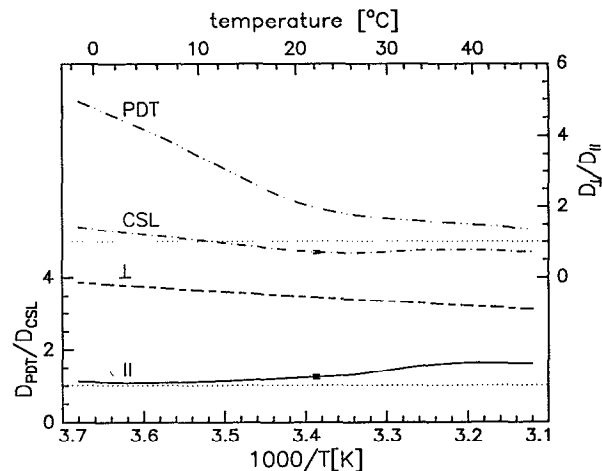
The anisotropy of diffusion is different for CSL and PDT, [cf. Fig. 3]. Plots of $D_\perp/D_\parallel$ vs temperature for both probes are shown in Fig. 4. For PDT, the ratio is always greater than one, i.e., diffusion of the globular PDT within smectic layers is always faster than traversing them. The opposite is observed for CSL: the ratio is less than one for most of the temperature range studied, but it increases to values above unity in the low temperature range of the smectic phase. Thus the cigarlike CSL shows greater ability to penetrate through the layers, than to move within them. For each probe the plot of $D_\perp/D_\parallel$ vs T shows a nonlinearity that reflects a transition in $D_\parallel$ from its low temperature to high temperature behavior, (cf. Figs. 3 and 4).

IV. DISCUSSION

Our results clearly demonstrate significantly different translational dynamics of PDT and CSL probes in the smectic phase of S2. But the most striking result is the rather abrupt change in the activation energy of $D_\parallel$ for both spin probes at a temperature around $t^* = 26$–27 °C, and this requires separate consideration. To aid in the interpretation of the present results, we have developed a model for the translational diffusion based upon the free volume concept. The discussion is divided into subsections.

TABLE I. Arrhenius law parameters and their standard deviations for translational diffusion of CSL and PD-Tempone in S2 and of methane in 8CB (E_a in kcal/mol, D_0 in cm²/s).

Geometry	$D_\perp$		$D_\parallel$			
			High T		Low T	
Spin probe	$E_\perp \pm \sigma_E$	$D_{0\perp} \pm \sigma_D$	$E_\parallel \pm \sigma_E$	$D_{0\parallel} \pm \sigma_D$	$E_\parallel \pm \sigma_E$	$D_{0\parallel} \pm \sigma_D$
CSL	9.2 ± 0.1	0.36 ± 0.04	9.0 ± 0.8	0.4 ± 0.2	14.0 ± 0.2	$(1.78 \pm 0.3) \times 10^3$
PD-Tempone	8.4 ± 0.1	0.33 ± 0.03	10.8 ± 0.5	10.3 ± 3.5	15.1 ± 0.3	$(12.6 \pm 3.3) \times 10^3$
Methane	4.7 ± 0.4		11.9 ± 0.4	Ref. 15		

First, we discuss the relative differences in the diffusion coefficient with respect to probe size and solvent orientational order. Second, the temperature dependence of the diffusion coefficients is addressed, including the anomalous behavior of $D_{\parallel}$. The last subsection summarizes the main predictions of the theory, and how they relate to the observations.

A. Anisotropy of diffusion coefficients

Given the very sparse information on translational diffusion in S2, we will compare our results with other results obtained in related cyanobiphenyls. It does not seem unreasonable to expect that the smectic A phase of the eutectic mixture S2, that is half 8CB with the other half a mixture of the related 10CB and 10OCB, to demonstrate many of the features characteristic of the pure cyanobiphenyls.

The diffusion coefficients measured by DID-ESR lie in a range that is similar to what is estimated from INS studies for self-diffusion in S2 and 5CB,[10,11] and from our 2D-ELDOR and ESE studies of $D_{\parallel}$ for CSL diffusing in S2.[29] However, Moseley and Loewenstein[15,17] obtained results on the diffusion of methane in 8CB by NMR, that are an order of magnitude faster. Similar differences between self-diffusion and probe-diffusion coefficients were also found for other liquid crystals.[15,17]

Let us first address the differences in the magnitude of D observed for CSL, PDT, and methane. It is convenient to consider the transverse diffusion (i.e., $D_{\perp}$), which is least influenced by the smectic order,[7] i.e., there is no significant change of $D_{\perp}$ at the N–S transition, so any differences in $D_{\perp}$ for different probes should be associated with probe size and orientational order rather than with the smectic layer structure.

To estimate the diffusion coefficient we make use of the well-known Stokes–Einstein relation for a spherical molecule of radius a diffusing in an isotropic medium of viscosity η,

$$D = \frac{kT}{\Xi} = \frac{kT}{6\pi\eta a}, \qquad (5)$$

where Ξ is the friction coefficient.

As described by Lamb,[38] Eq. (5) also holds for an ellipsoid diffusing in an isotropic medium, but a has to be replaced by the equivalent hydrodynamic radius a_i. This radius depends on the orientation of the ellipsoid with respect to the direction of diffusion. Assuming that the asymmetric probe is a prolate ellipsoid with semiaxes $[b:b:c](c > b)$ we find

$$a_t = \frac{8}{3} \cdot \frac{1-x}{\chi_0(2-3x)+1} \cdot c, \qquad (6)$$

for diffusion transverse to the prolate long axis, and

$$a_l = \frac{8}{3} \cdot \frac{1-x}{\chi_0(2-x)-2} \cdot c, \qquad (7)$$

for diffusion parallel to the long axis; $x = (b/c)^2$ and $\chi_0 = \ln\{[1+(1-x)^{1/2}]/[1-(1-x)^{1/2}]\}/(1-x)^{1/2}$.

For the general case of a prolate molecule diffusing in a liquid crystalline medium with anisotropic viscosity, then

η in Eq. (5) should be the component characteristic of the geometry of the diffusion, i.e., η_i, $i = \parallel$ or $\perp$. In the absence of theoretical predictions, these two hypothetical viscosities should probably be associated with two of the Miesowicz viscosities,[39–41] namely, $\eta(\mathbf{n}\parallel\mathbf{v})$ and $\eta(\mathbf{n}\parallel \text{grad}|\mathbf{v}|)$, respectively; $\mathbf{n}$ and $\mathbf{v}$ are the nematic director and the flow velocity vector, respectively.

We begin with a comparison of the diffusion of the globular methane and PDT molecules, since both are more or less spherical, and their coupling to the medium should be qualitatively similar. From Eq. (5) it follows that for a spherical probe diffusing in a nematic solvent the diffusional anisotropy measured by the $D_{\perp}/D_{\parallel}$ ratio is determined just by the solvent anisotropy (i.e., η_i). If two probes (labeled "1" and "2") are diffusing in the same geometry, one finds from the appropriately modified Eq. (5) that

$$D_{1,j}/D_{2,j} \propto a_2/a_1, \quad j = \parallel \text{ or } \perp, \qquad (8)$$

Methane is to a very good approximation a spherical molecule with radius of about 1 Å, but PDT is a slightly prolate axially symmetric ellipsoid with $[b:b:c] = [3.8:3.8:5.6]$ Å.[42] However, since this anisotropy is not large, and since PDT is reorienting as it translates, we will consider it as spherical with an average equivalent radius of $a_{\text{PDT}}^{\text{av}} \approx 4.32$. From Eq. (8) one finds that $D_{\text{meth},\perp}/D_{\text{PDT},\perp} \propto a_{\text{PDT}}^{\text{av}}/a_{\text{meth}} \approx 4.32$, and this result deviates substantially from the experimental finding at room temperatures, cf. Table I and Refs. 15 and 17. Significant discrepancies are to be expected given the nearly factor of 2 difference in the activation energies for methane and PDT: 4.7 and 8.4 kcal/mol, respectively. Such a difference, in our opinion, reflects the different local environments both probes are residing in, and, therefore, the different viscosities they experience. Methane is probably located primarily in the highly fluid aliphatic region, whereas PDT, although (partially) expelled from the hard-core region is still significantly interacting with it, cf. next subsection.

The slow diffusion of CSL is expected, since this probe is a rigid body with a similar length to that of the fully extended cyanobiphenyls that constitute S2.[43] The hydrodynamic size of CSL is, therefore, significantly larger than for PDT, and this increases the viscous drag. CSL also experiences a noticeable anisotropy when diffusing transverse vs. parallel to its long axis, even in isotropic medium. In the perfect ordering limit, we can equate molecular l, t axes with the laboratory $\parallel$, $\perp$ axes. Then the diffusion coefficients can be estimated from the modified Stokes–Einstein equation. Given the high ordering of CSL in S2 ($S = 0.6$–0.8),[13] the use of this limit would appear to be a reasonable aproximation.

Using Eqs. (6) and (7) to calculate the equivalent radii for CSL with semiaxes $[b:b:c] \approx [4:4:16]$ Å,[44] we find that $a_t \simeq 8.21$, and $a_l \simeq 6.37$, and one can use these values in conjunction with Eq. (5) to estimate D in the smectic phase. With the aid of Eq. (5) we get $D_{\text{PDT},\perp}/D_{\text{CSL},\perp} \approx 1.9$, and this value is a factor of about 2 smaller than the experimentally observed $3 < D_{\text{PDT},\perp}/D_{\text{CSL},\perp} < 4$, cf. Fig. 4.

Again, we may argue that this difference results from a difference in the viscosities both probes experience, which also manifests itself in the slightly different activation energies, cf. Table I.

Since $D_\parallel / D_\perp > 1$ for CSL at high temperatures, a feature characteristic of the nematic phase, whereas this ratio is less than one for the small probes, it is instructive to see if this can be explained by simple geometric considerations. From Eq. (5), for the isotropic viscosity case, one obtains $D_{CSL,\parallel}^{iso} / D_{CSL,\perp}^{iso} \approx 0.8$. However, we can correct this result for the anisotropic viscosity. For the nematic phase of 5CB and 8OCB cyanobiphenyls, the Miesowicz viscosity ratio, $\eta(\mathbf{n}\parallel \mathbf{v})/\eta(\mathbf{n}\parallel \text{grad}|\mathbf{v}|)$, is about 0.5,[45,46] and we obtain $D_{\parallel \text{ nem}}^{CSL}/D_{\perp \text{ nem}}^{CSL} \approx 0.4$, which is in good agreement with the experimental findings in Fig. 3 and Fig. 4.

Note that a different method of estimating of $D_\perp / D_\parallel$ was suggested by Chu and Moroi,[47] which is based on the assumption that diffusion occurs in perfectly ordered clusters of molecules. Instead of using the Stokes–Einstein equation, they estimate the anisotropy ratio in the perfect order limit, $D_\perp^0 / D_\parallel^0 \approx b/c$, by calculating the frequency with which the probe finds its path through a unit area perpendicular to the direction of diffusion. Note, that this frequency plays the role of the $a\eta$ term in the denominator of Eq. (5). On transforming the diffusion tensor from the cluster frame to the laboratory frame they found for the nematic phase

$$D_\perp / D_\parallel = \frac{(1-S)+(2+S)(D_\perp^0/D_\parallel^0)}{(1+2S)+2(1-S)(D_\perp^0/D_\parallel^0)}, \qquad (9)$$

where S is the order parameter. Eq. (9) was developed for the case of self-diffusion, but can be used for any probe, (cf. Ref. 47), if one takes b/c to be that for CSL, but the order parameter is that of S2, cf. Ref. 47. For S in the range of 0.5 to 0.6, and $b/c=0.25$ we obtain from Eq. (9) $D_{CSL,\perp} / D_{CSL,\parallel} \approx 0.4$, in agreement with the previous result.

The nematiclike behavior of the diffusional anisotropy of CSL in S2 is also illustrated by the very similar activation energies for $D_\perp$ and $D_\parallel$ at high temperatures, cf. Table I. Thus there appears to be no hint of any role of the smectic phase translational potential barrier to the activation energy for $D_\parallel$ [cf. Eq. (11) below]. These results indicate that the CSL spin probe is only very weakly (if at all), coupled to the smectic bilayer structure for temperatures above t^*.

This inference raises a question about the equilibrium position of CSL in the smectic bilayer phase, especially given the high degree of orientational order of CSL in S2, guaranteeing that the probe is strongly coupled to the director.[29] The bilayer structure of the smectic A phase of cyanobiphenyls is characterized by a spacing $d \simeq 1.4l$, l being the molecular length, with a weakly defined hard-core region of the bilayer.[48,49] Close to the smectic-nematic transition a hard-core region is hardly distinguishable, and this, together with the fact that the length of CSL is comparable to l, should result in CSL extending the length of a bilayer. Its center need not reside in any precise location relative to the ill-defined hard-core region, and it may extend between two bilayers, but its environment, integrated

over its length is about the same. This would mean that its orientational ordering is largely independent of its precise location relative to the hard-core region. However, the smaller methane and PDT, as well as the cyanobiphenyl molecules, because they are only partially rigid, would favor a precise location within the layer structure, i.e., experience a translational potential. The unique feature of CSL could disappear as the layer structure becomes better defined and CSL takes on a prefered location; this is what probably happens below t^*.

B. Temperature dependence of diffusion

It is well known from previous studies,[14] that insight into the role of smectic order on translational motions of probes, may be inferred from the temperature variations of the diffusion coefficients. Volino and Dianoux[50] and Moro *et al.*[51,52] have independently shown that the longitudinal diffusion of a small globular probe over times that are long compared to the time of traversing a single smectic layer, can be described as a random jump over the barrier of the hard-core region of the smectic layer. Since the transverse diffusion is not affected by the translational ordering with respect to the longitudinal direction, they found[51]

$$D_\perp = D_\perp^0 \exp[-E_\perp/kT], \qquad (10)$$

$$D_\parallel = D_\parallel^0 (\Delta/kT)\exp[-(E_\parallel+\Delta)/kT], \qquad (11)$$

where it is assumed that the translational potential due to the layering is of form: $U(z) = -\frac{1}{2}\Delta \cos(2\pi z/d)$, where d is the layer spacing. Equation (11) expresses the fact that diffusion parallel to the director requires the small globular probe to overcome not only the viscous drag of the medium but also the potential barrier. Despite the simplifying assumption of a cosine translational potential, it does lead to a reasonable dependence of the activation energy for $D_\parallel$ on this potential.

To get further insight into the relation between smectic ordering, probe size, and the activation energy for diffusion, we developed a model based on the free-volume theory, which is presented in detail in Appendix A. The basic assumption of the model is that each molecule spends most of its time rattling inside a cage formed by its neighbors. Any substantial displacement of the molecule happens only after density fluctuations enlarge the cavity size sufficiently. Substantial translation occurs not as a result of an activation process in the usual sense, but rather as a result of the redistribution of the free volume within the liquid. In the model the cage expansion is related to the smectic phase free energy, the local compressibility k_z, and the probe length, l, with respect to the interlayer distance, d, as measured by the ratio l/d. The smectic potential used by the theory is of the McMillan type.[53] In this way, the local diffusion coefficient, $D(z)$, (i.e., the value of D when the probe has an instantaneous position of z along the normal to the layer), becomes sensitive to the smectic potential acting on the diffusing probe, and to the local compressibility. To facilitate the model development we made an assumption that the solvent and probe molecules are rigid rods with the same diameter. However, to the extent that

the hydrodynamic radius of the probe scales the magnitude [cf. Eq. (5)] and not the temperature dependence of the diffusion coefficient, the results of the free-volume theory would also be applicable to smaller probes.

To obtain the macroscopic diffusion coefficient of interest, the local diffusion coefficient $D(z)$, is averaged appropriately along the particular direction of diffusion. As a result, the activation energy for the macroscopic $D_\perp$ is a function of the smectic phase order parameters: $S = \langle P_2(\cos\theta)\rangle$ (i.e., the orientational order parameter), $\sigma = \langle P_2(\cos\theta)\cos(2\pi z/d)\rangle$ (i.e., the orientational-translational order parameter), and $\gamma = \langle\cos(2\pi z/d)\rangle$ (i.e., the translational order parameter), and is dependent upon where the probe prefers to reside within the layer (i.e., on the probe order parameters S_p, σ_p, and γ_p, and as well as the relevant average compressibility $\langle k\rangle$).

The derivation of the macroscopic $D_\parallel$ is based on a somewhat different approach from that of Moro and Nordio.[51,52] We consider continuous diffusion across the smectic layers, and the averaging of $D(z)$ is done via estimation of the average friction coefficient Ξ (in units of kT) acting on the diffusing molecule, cf. Eq. (5). As a result, the dependence of the activation energy on the smectic order parameters of the solvent and the compressibility across the smectic layer is obtained, cf. Appendix A.

Let us again first consider globular probes. We find that for transverse diffusion of PDT and methane in cyanobiphenyls, the activation energy of $D_\perp$ (T) for methane is nearly half that of PDT, cf. Table I and Ref. 15. This difference probably results from the fact that both probes reside in different parts of the smectic bilayer. Methane presumably resides mostly in the most fluid aliphatic part of the smectic layer,[15,17] whereas PDT remains somewhat closer to the hard core of the bilayer due to dipolar attractions; (both S2 and PDT are polar molecules). Steric interactions do tend to expel PDT from the hard-core regions, but nevertheless the probe exhibits some degree of orientational and translational ordering. Typical values are $S_{PDT}\sim 0.2$, $\sigma_{PDT}\sim 0.15$, and $\gamma_{PDT}\simeq 0.3$ in S2.[29] The observed difference in activation energies can be rationalized in terms of our free-volume model. For convenience, let us introduce the normalized "excess activation energy," $\Delta\mathscr{E}$, by which the activation energy for diffusion in the isotropic phase, β_p, is augmented by the presence of the orientational and translational order. For transverse diffusion, from Eq. (A26) we write

$$\Delta\mathscr{E}_\perp = (E_\perp - \beta_p)/\vartheta_0 = \langle k\rangle[SS_p + \Lambda_p\sigma\sigma_p + \epsilon_p\Lambda_p\gamma\gamma_p],$$
$$\tag{12}$$

where subscript "p" refers to the probe molecule; Λ_p and ϵ_p are parameters of the smectic potential experienced by the diffusing probe [cf. Eq. (A5)]; $\langle k\rangle$ is the average compressibility of the smectic phase, and ϑ_0 is a factor proportional to the smectic potential depth, U_0, cf. Eq. (A16) and Ref. 53.

We assume that methane has a negligible orientational order but significant translational order leading to its location in the aliphatic chain region (i.e., $\langle z\rangle\approx d/2$). That is, $S_{meth}\simeq 0$, $\sigma_{meth}\simeq 0$, and $\gamma_{meth} < 0$. It follows from Eq. (12)

that $\Delta\mathscr{E}_{meth,\perp} = \langle k\rangle\epsilon_{meth}\Lambda_{meth}(0)\gamma\gamma_{meth} < 0$, i.e., a *negative* excess energy! This implies that $E_{meth,\perp}$ should be *smaller* than the activation energy for diffusion in the isotropic phase, as indeed is observed experimentally, i.e., 4.7 and 6.6 kcal/mol, respectively (cf. Table II of Ref. 15). For PDT on the other hand, typical values of all the order parameters are nonzero and positive, as given above, so $\Delta\mathscr{E}_{PDT,\perp} > 0$. That is, the smectic order enhances $E_{PDT,\perp}$ compared to the isotropic phase. Therefore, the experimental finding of $E_{PDT,\perp} > E_{meth,\perp}$ (cf. Table I) is explained by the free-volume theory.

Despite this difference in $E_\perp$, the *diffusional anisotropy* for the small methane molecule and for the larger oblate PDT show similarities; compare the present Fig. 3 with Fig. 7 of Ref. 15. This is a consequence of the expulsion of both globular probes from the hard-core region. For both probes the diffusion within the smectic layers is faster than across them, with $E_\perp < E_\parallel$. Comparison of $D_\parallel$ and $E_\parallel$ for methane vs PDT suggests that although $D_{meth,\parallel} > D_{PDT,\parallel}$, the activation energies obey $E_{meth,\parallel} > E_{PDT,\parallel}$. Thus since $E_{meth,\perp} < E_{PDT,\perp}$, it follows that the ratio $E_\parallel/E_\perp$ is much larger for methane than for PDT. These findings are clearly associated with the structure of the smectic A phase. The excess activation energy for $D_\parallel$ is

$$\Delta\mathscr{E}_\parallel = (E_\parallel - \beta_p)/\vartheta_0$$
$$= k^{max}\{(1+\delta_S)[S + \Lambda_p\sigma]\cdot S_p^0 + \epsilon_p\Lambda_p\cdot\gamma\}, \tag{13}$$

where k^{max} is the compressibility of the hard-core region, and S_p^0, and δ_S denote, respectively, the mean order parameter of the probe, and the amplitude of its variation across the layer, cf. Eq. (A27) and Appendix A. For typical values of order parameters of methane and PDT one gets $\Delta\mathscr{E}_\parallel^{meth}\simeq k^{max}\epsilon_{meth}\Lambda_{meth}\gamma$ for methane, and $\Delta\mathscr{E}_\parallel^{PDT}\simeq 0.4k^{max}(S + \Lambda_{PDT}\sigma) + k^{max}\epsilon_{PDT}\Lambda_{PDT}\gamma$ for PDT; (assuming $\delta_S = 1$, i.e., PDT is completely decoupled from the orientational order when in the center of the aliphatic region[29]). $\epsilon_{meth}\Lambda_{meth}$ is probably somewhat larger than $\epsilon_{PDT}\Lambda_{PDT}$, since methane experiences a deeper translational potential well. Thus to the extent that the γ-dependent term is the largest for $\Delta\mathscr{E}_\parallel^{meth}$, the excess activation energy of methane is expected to be slightly larger than or comparable to that of PDT, cf. Fig. 5. The experimentally observed values, $E_\parallel^{meth}\simeq 11.9$ kcal/mol, and $E_\parallel^{PDT}\simeq 10.8$ kcal/mol (high temperatures) or 15.1 kcal/mol (low temperatures) agree reasonably with this estimation, cf. Table I.

We note in this respect, that the anisotropy of electrical conductivity in cyanobiphenyls is qualitatively very similar to the diffusional anisotropy of PDT and methane. The conductivity, which is directly related to the charged impurity diffusion, $\sigma\sim D/RT$, was studied in 8OCB by Mircea-Roussel *et al.*,[54] and in 8CB Jadzyn and Kedziora.[55] It was found in 8CB that $\sigma_\perp\gg\sigma_\parallel$ and $E_{\sigma,\parallel}\simeq 19.6$ and $E_{\sigma,\perp}\simeq 15.7$ kcal/mol.[55] The fact, that the activation energies for conductivity are relatively high is probably due to strong interactions between charge carriers and polar cyano groups of liquid crystalline molecules that enhances the translational potential well (a larger $\epsilon\Lambda$ factor).

It is somewhat surprising to find that the $E_\perp$ for CSL is only slightly higher from that for PDT, cf. Table I. However, consideration of excess activation energies resulting from the free-volume theory shows that for typical values of the smectic order parameters of S2 and both probes, such a situation is quite possible, cf. Fig. 5. For a long probe like CSL, because it is to a large extent decoupled from the translational order, the Λ_{CSL} is very small, and the dominant factor in the excess activation energy will be the SS_{CSL}^0 term, cf. Eq. (12). For PDT, Λ_{PDT} must be significant since the probe is expelled from the hard-core region, but since order parameters are small, all terms in Eq. (12) are small and similar in magnitude. Results of the sample numerical calculation shown in Fig. 5 demonstrate that for reasonably chosen values of the parameters indeed $\Delta\mathscr{E}_{PDT,\perp} \lesssim \Delta\mathscr{E}_{CSL,\perp}$ can be observed.

A pronounced change of the slope in the log $D_\parallel$ vs $1/T$ plot around t^* for either PDT or CSL diffusion is the most unusual feature of the present studies, cf. Fig. 3. It is not observed in $D_\perp$, which exhibits simple Arrhenius behavior. The feature seems to be unique for S2 since it was not previously observed in any smectic phase.[14] The observed abrupt change in $E_\parallel$ at t^* does correlate with the results of our studies of the dynamics of PDT in S2 by means of 2D-ELDOR and electron spin echoes.[29] We estimated the temperature dependence of the rotational correlation time, τ_R, of PDT, and it also featured a noticeable change around t^*, (cf. Table II of Ref. 29). Despite substantial uncertainty in τ_R values, it was found that τ_R drops by about factor of 2 as the temperature decreases below t^*.

A possible explanation of these observations is as follows. Transverse diffusion of PDT in S2 is dominated by its behavior in the aliphatic region. That is, at all temperatures in the smectic phase the effective $D_\perp$ results from diffusion in the aliphatic region, because even though PDT can have finite probability near the hard-core region its, $D_\perp(z)$ in that region is small. However, rotational reorientation occurs effectively for all values of z even though $\tau_R = \tau_R(z)$. Thus if there is some subtle change or rearrangement in the hard-core region of the bilayer, the observed $D_\perp$ would hardly be affected, whereas the observed τ_R would be. $D_\parallel$ would have to be affected because it necessarily involves passage through the hard-core region. Cyanobiphenyls are known to undergo dimer associations, especially as the temperature is reduced.[56] We may assume that at high temperatures hopping through the layer is more frequent because the bilayer is poorly defined and the number of dimers is relatively low, yielding a smaller barrier. At lower temperatures, the hard-core of the bilayer packed with dimers becomes more dense and better defined, and this would augment the apparent barrier. In our free-volume model such an effect would correspond to changes first of all in Λ_p and the compressibility, cf. below.

$D_\parallel$ for CSL should also be affected by the same process leading to a similar change in activation energy. Indeed, CSL also exhibits a transition from nematiclike diffusion above t^* (where $D_\parallel/D_\perp > 1$), to smecticlike diffusion (where $D_\parallel/D_\perp > 1$) below, as a result of an increase in activation energy comparable to that experienced

by PDT. Thus $D_{CSL,\parallel}$ becomes somewhat similar to $D_{PDT,\parallel}$, in their respective smecticlike behavior (cf. Fig. 3 and Table I).

The relative magnitudes of the activation energies obtained from the experiment are also consistent with our model. For the high temperature smectic phase we found $E_\parallel$ for PDT being little greater than for CSL. For l/d typical for PDT (0.2–0.3) and for CSL (0.6–0.8) one finds from Fig. 5, that such a relation between the $\Delta\mathscr{E}_\parallel$ can be obtained only for a "soft" smectic phase, (cf. curve -△- in Fig. 5). This supports our suggestion concerning the smectic phase above t^*; for weak smectic order the free volume model predicts $E_{long,\perp} \gtrsim E_{short,\perp}$, $E_{long,\parallel} \lesssim E_{short,\parallel}$, and $[E_{long,\parallel} - E_{long,\perp}] < [E_{short,\parallel} - E_{short,\perp}]$, as is observed for CSL and PDT above t^*, cf. Table I.

Below t^*, $E_\parallel$ for PDT and CSL abruptly increase by factors of 1.40 and 1.56, respectively, presumably due to the better defined translational ordering. From Fig. 5, one can find, for example, that by moving from a case of a "soft" to "hard" smectic phase, cf. △ vs ▲ curves in Fig. 5, the activation energy becomes larger, and this enhancement should be somewhat more pronounced for the short than for the long probe. From Table I we find that within experimental error, the difference in the activation energies below and above t^*, are, however, comparable, i.e. $[E_{PDT,\parallel}^{low} - E_{PDT,\parallel}^{high}] \approx [E_{CSL,\parallel}^{low} - E_{CSL,\parallel}^{high}]$. But one still concludes that the low temperature smectic phase is more highly ordered.

In the absence of other experimental evidence the coupling between diffusion and monomer–dimer association in the bilayer structure that is suggested above is a speculative one. However, we would like to point out that very similar deviations from Arrhenius behavior of transport and relaxation coefficients such as shear viscosity, self-diffusion, and T_1 nuclear spin relaxation have been observed in polar liquids like picolines and pyridine, as well as toluene.[57] It is interesting, that some of these deviations were not accompanied by any specific heat anomalies, suggesting changes in dynamical processes without any sharp structural changes. Two different explanations were offered: (i) restrictions of the freedom of rotation about some of the molecular axes; and (ii) various kinds of association of the molecules in the liquid state. The latter is very much in line with our suggestion.

Finally we wish to address the fact that the sharp change in $E_\parallel$ arround T^* is accompanied by a dramatic change of the pre-exponential factor in the fit of an Arrhenius law. Although this behavior is common at phase transitions, as witnessed in a variety of molecular dynamics studies, (e.g., for liquid crystals Refs. 14, 15, and 27), to our knowledge it has not been adequately addressed. In fact, the preexponential factor is usually merely considered as a scaling factor. While we are not able at present to clarify the matter, we do wish to note that the free volume theory might offer a solution to the problem. The pre-exponential factor in the free volume theory, cf. Eq. (A2), is a product of $g(V^*)$ a geometrical factor that depends on

the size of the critical free volume, V^* sufficient for a substantial displacement, and $\mathscr{D}^0$, the in-cage diffusion constant. For a given system, any substantial changes in the preexponential factor are due to changes in g, since $\mathscr{D}^0$ is diffusion in the absence of the cage. Note that $g > 1$, which accounts for the faster decay of the momentum autocorrelation function in the cage-limited space, and the dependence of g on the cage size can be dramatic, by analogy to what is observed for spatially restricted rotational diffusion.[58]

In developing the free volume theory along the lines of Cohen and Turnbull,[59] we did not consider any particular shape for the cage, assuming only that it is sufficient for a significant jump of the probe. Consequently, the cage shape and the value of g remain unspecified in the model. We believe that the dramatic jump in value of the preexponential factor of $D_{\parallel}$ in Table I, can at least to some extent, be explained by a change in the value of g at t^* due to a transition from a poorly to well defined bilayered structure of the smectic phase, a matter we wish to study in the future.

C. Further predictions from the free-volume theory

In the previous section we used our free-volume model to rationalize the observed differences in activation energies for the different probes and for the two basic geometries of diffusion in the smectic phase of cyanobiphenyls. We now wish to consider some general predictions of the dependence of the activation energy on the ordering of the smectic solvent and of the probe, and of the ratio of the probe length to smectic interlayer distance, l/d.

In order to get some insight, detailed calculations were performed for reasonable values of the smectic order parameters, using results of our earlier studies of PDT and CSL in S2.[29] Thus order parameters of the smectic phase of S2 were taken to be $S = 0.8$, $\sigma = 0.6$, and $\gamma = 0.75$. The dependence of the probe order parameters on l/d were approximated by monotonic functions. For example, it is well known that the orientational order parameter, S_p of a probe increases with l/d. We took this functional dependence to be approximated by $\tanh[a(l/d - 0.1)]$. This yields $S_p = 0$ for $l/d = 0.1$, nearly linear variation of S_p with l/d in the range (0.2–0.8) and an asymptotic increase to unity for $l/d \gg 1$. A value of $a = 1.35$ was chosen such that $S_p \approx 0.2$ for $l/d = 0.2$ and $S_p \approx 0.8$ for $l/d = 0.8$, the values characteristic of PDT and CSL in S2, respectively.[29] Similarly, the translational and rotational–translational order parameters, γ and σ, were approximated by arbitrarily chosen functions, normalized such that for $l/d = 0.2$ (PDT) $\sigma_p = 0.15$, and $\gamma_p = 0.3$, and for CSL probe with $l/d = 0.8$, $\sigma_p \approx \gamma \approx 0$. However, the latter choice is not crucial since the activation energy predicted for a long probe is not very sensitive to these order parameters, e.g., the activation energy changes only slightly when their values are increased to $\sigma_p = \gamma_p = 0.2$.

For simplicity, the functional form of $\Lambda_p(l/d)$ was adopted following McMillan, who used it for modeling the phase transitions with somewhat different meaning of l/d,
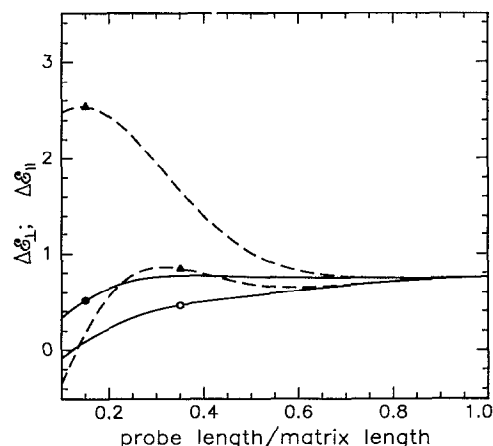

FIG. 5. Calculated normalized excess activation energies for longitudinal (– – – –) and transverse (—) diffusion as a function of the ratio l/d, for $S = 0.8$, and $k_0 = \langle k \rangle = 1$. The curves correspond to the following sets of parameters: (open symbols) $\sigma = 0.3$, $\gamma = 0.375$, $\epsilon_p = 0.5$, $\lambda_p = 2.0$ and (full symbols) $\sigma = 0.6$, $\gamma = 0.75$, $\epsilon_p = 1.5$, $\lambda_p = 3.0$.

i.e., $\Lambda_p(l/d) = \lambda_p \exp[-q(l/d)^2]$,[53] although we let λ_p vary (but we set $q = 1$ for simplicity).

In Fig. 5 we present a comparison of the excess activation energies $\Delta\mathscr{E}_i$ vs l/d [$i = \parallel$, and $\perp$, cf. Eqs. (13) and (12)], for two different sets of ϵ and λ_p, and for two significantly different values of the compressibility variation across the smectic layer. That is, δ_0 [cf. Eq. (A7)] was arbitrarily set to be proportional to Λ $(\sigma S + \epsilon\gamma)$ (cf. Appendix A), with $\Lambda = 0.12$ and $(\sigma; \gamma) = (0.3; 375)$ or $(0.6; 75)$ with proportionality constants of 1 or 2, respectively.

The following qualitative conclusions may be drawn from Fig. 5. The $\Delta\mathscr{E}_{\parallel}$ for long probes ($l/d > 0.6$) is essentially insensitive to the smectic potential parameters of the probe, λ_p and ϵ_p, and it is only weakly dependent on the compressibility. Both features signify effective decoupling of the probe from the translational part of the potential. For a small probe ($l/d < 0.4$), $\Delta\mathscr{E}_{\parallel}$ increases significantly with increase in the translational ordering of the probe, and the effect is stronger the better defined the smectic structure, i.e., a larger amplitude of the compressibility wave, δ_0. For very small probes, the activation energy decreases, and this reflects the fact that the probe easily finds its way through the hard-core region; (i.e., smaller fluctuations in the environment are required to substantially increase the probe's free volume).

For transverse diffusion, the long probe is again essentially insensitive to the smectic translational ordering and compressibility. Note at this point, that for such a probe the $\Delta\mathscr{E}_{\parallel}$ and $\Delta\mathscr{E}_{\perp}$ activation energies are practically the same, a feature most characteristic for the nematic phase.[14] The $\Delta\mathscr{E}_{\perp}$ decreases slowly with probe length as it decreases to $l/d \approx 0.2$. For a very short probe the situation is different: $\Delta\mathscr{E}_{\perp}$ vs l/d drops rapidly as l/d is decreased.

The very weak dependence of $\Delta\mathscr{E}_{\perp}$ on the smectic ordering of the probe, and on the probe length is consistent with the experimentally observed similarity in $\Delta\mathscr{E}_{\perp}$ for different length probes. For longitudinal diffusion the

model anticipates a wide range of behaviors, from similar $\Delta\mathscr{E}_{\parallel}$ for short and long probes in the limit of "soft," ill-defined smectic layers, to $\Delta\mathscr{E}_{\parallel}^{\text{short}} > \Delta\mathscr{E}_{\parallel}^{\text{long}}$ for "hard," well-defined smectic layering. When we compare the calculations with the experimental results for diffusion of PDT and CSL in the smectic A phase of S2, we again note that reasonable agreement can be obtained from our model if the smectic phase under investigation is a soft one at high temperatures, but becomes better defined deep in the smectic phase, as we expect.

ACKNOWLEDGMENTS

APPENDIX A: THE FREE-VOLUME MODEL OF TRANSLATIONAL DIFFUSION IN THE SMECTIC PHASE

The principal concept of the free-volume model is that each molecule of a system is confined to a cage by its neighbors. The molecule is rattling inside this volume until fluctuations in density open up a hole within the cage large enough to permit a substantial translation of the molecule. Thus the large scale displacement occurs not as a result of an activation in the ordinary sense but rather as a result of redistribution of the free volume within the liquid.

Introducing two characteristic free volumes, a critical free volume volume V^*, large enough to permit a substantial displacement, and V^f, the average free volume per molecule, the diffusion coefficient can be expressed as[59]

$$\mathscr{D} \simeq \tilde{\mathscr{D}}(V^*)e^{-\zeta V^*/V^f}, \tag{A1}$$

where $\tilde{\mathscr{D}}(V^*)$ is the "in cage" diffusion coefficient in a cage of volume $(V^* + \bar{V})$ with $\bar{V}$ the mean molecular volume. Since the average free volume can be assumed to arise from the isobaric thermal expansion, Eq. (A1) can be rewritten as

$$\mathscr{D} = g(V^*)\mathscr{D}^0(T)e^{-\beta/(T-T_0)}, \tag{A2}$$

where $\beta = \zeta\delta V/\alpha\bar{V}$, $\delta V = V^* - V^f$, α is the mean value of the thermal expansion coefficient and T_0 is the temperature at which the volume per molecule would be reduced to the close-packing limit. $\mathscr{D}^0(T)$ is the small-scale diffusion constant, $g(V^*)$ is a numerical factor related to the size of the cage, such that $\tilde{\mathscr{D}}(V^*) = g(V^*)\mathscr{D}^0(T)$. ζ is a numerical constant.

Equation (A2) was developed for a simple liquid of hard spheres by Cohen and Turnbull,[59] and was successfully applied to explain the fluidity of a large number of glass-forming substances.

Diogo and Martins have used a similar approach to explain the temperature dependence of the twist viscosity in the nematic phase,[60] and we have used such an approach to obtain a model explaining the temperature dependence of transverse diffusion in mixed model membranes,[24] which

may be regarded as lyotropic smectic phases. In that work we considered diffusion of probes which very closely resemble the lipid and cholesterol components of the membranes. Since we were at that time concerned only with the transverse (or lateral) diffusion coefficient ($\mathscr{D}_{\perp}$), it was then sufficient to account only for the presence of the orientational order in the smectic layer. Here the free-volume theory is reconsidered in order to fully account for the smectic order and to estimate activation energies for longitudinal and transverse diffusion from a common approach. To make the theory applicable to a variety of probes ranging from globular ones of the size of PDT as well to rigid and elongated ones like CSL, let us consider a probe of arbitrary length l, and for simplicity the same diameter as the liquid crystalline molecule. This ensures that all characteristic volumes for the probe, $\{V_p\}$ are simply proportional to the corresponding characteristic volumes of the liquid crystalline molecule $\{V_{\text{lc}}\}$, as well as that intermolecular interactions (per unit length) are the same. Since the model is designed primarily to account for the activation energy, we may argue that despite this simplification it is also applicable to probes with sizes that depart significantly from the liquid crystalline molecule, i.e., for relatively very small probes like methane or oxygen, or bulkier like tetramethylsilane; the probe size primarily affects the magnitude of the diffusion coefficient, and not the activation energy, cf. the Stokes–Einstein relation, Eq. (5).

Diffusion in the isotropic phase of the liquid crystalline material is taken as the reference. The critical free volume for a probe in the isotropic phase is defined as V_{iso}^* $= V_{\text{iso}}^f + \delta V$, where V_{iso}^f is an average free volume per molecule and δV is an increase in the free volume sufficient for the displacement. The translational diffusion coefficient is then given by Eq. (A2) with $V^* \equiv V_{\text{iso}}^*$ and $\mathscr{D}^0(T)$ $\equiv \mathscr{D}_{\text{iso}}^0(T)$,

$$\mathscr{D}_{\text{iso}}(T) = g_{\text{iso}}\mathscr{D}_{\text{iso}}^0(T)e^{-\beta_{\text{iso}}/(T-T_0)}, \tag{A3}$$

where $\beta_{\text{iso}} = \zeta \cdot \delta V/(\alpha_{\text{iso}}\bar{V}_{\text{iso}})$, $\mathscr{D}_{\text{iso}}^0(T)$ is the small scale diffusion coefficient in the isotropic phase, and $\bar{V}_{\text{iso}}$ is now the mean molecular volume per molecule in the isotropic phase.

The most pronounced and important feature of the smectic A phase is the existence of significant orientational and translational order of the liquid crystalline molecules. This smectic order is often considered as resulting from a mean field ordering pseudopotential experienced by each liquid crystalline molecule. The potential is usually assumed be of the form

$$U(\theta,z) = -U_0^{\text{sm}}[S + \Lambda(r_0/d)\sigma\cos(2\pi z/d)]P_2(\cos\theta)$$
$$+ \epsilon\Lambda(r_0/d)\gamma\cos(2\pi z/d)], \tag{A4}$$

which was first proposed by McMillan.[53] In Eq. (A4) θ is the angle between the long axis of the molecule and the director $\mathbf{n}$, and z defines the position of the center of mass of a liquid crystalline molecule with respect to the smectic layer (i.e., along the normal to the smectic layer).

S, σ, and γ are the smectic phase order parameters; $S=\langle P_2(\cos\theta)\rangle$ is the orientational order parameter, $\sigma=\langle P_2(\cos\theta)\cos(2\pi z/d)\rangle$ is the orientational-translational order parameter, and $\gamma=\langle\cos(2\pi z/d)\rangle$ is the translational order parameter, where the thermal average $\langle\cdots\rangle$ is as usual given by

$$\langle\cdots\rangle=\int_0^d dz\int_0^\pi \cdots P(\theta,z)\sin\theta\,d\theta,$$

where $P(\theta,z)=\exp[-U(\theta,z)/kT]/\int_0^d dz\int_0^\pi \sin\theta\,d\theta$ $\times\exp[-U(\theta,z)/kT]$ and U_0^{sm}, $\Lambda(r_0/d)$ and ϵ are smectic potential parameters, and it is assumed that $\Lambda(r_0/d)$ monotonously decreases with the ratio between r_0, which is of order of the hard-core part of molecule, and d, the interlayer distance.

To make Eq. (A4) applicable to the probe molecule, we assume that the concentration of the solute is so low that the order parameters of the solution are the same as of the pure liquid crystal. The form of Eq. (A4) would then hold for the probe, with r_0 being replaced by the length of the probe, l. That is,

$$U(\theta,z)=-U_0[S+\Lambda_p(l/d)\sigma\cos(2\pi z/d)]P_2(\cos\theta)$$

$$+\epsilon_p\Lambda_p(l/d)\gamma\cos(2\pi z/d)], \tag{A5}$$

where now θ, and z refer to the probe molecule, U_0, $\Lambda_p(l/d)$, and ϵ_p are the probe potential parameters, but the order parameters S, σ, and γ are of the smectic phase. We note that $\Lambda_p(l/d)$ in Eq. (A5) would also be a decreasing function of l/d. That is, a very small probe for which $l/d\ll 1$ will be a very effective probe of the z dependence of the potential, since over its length l this potential is nearly constant. But in the opposite limit of $l/d\gg 1$ the probe is so long that it always sees the average $\langle\cos(2\pi z/d)\rangle=0$ independent of the precise location with respect to z of its center of mass.

The ordering of the long molecular axis and of the center of mass result in the average free volume at the disposal of a molecule being (i) changed and (ii) position dependent. Therefore, following our earlier arguments,[24] if the probe located at z is to gain the critical free volume $V_p^*(z)$ for a translational jump, the cage has to expand, first by the amount it was changed by the transition from the isotropic to smectic phases $\Delta V_p^*(z)$, and, additionally by δV, to reach the size of V_{iso}^*, which is needed for the displacement. This can be written as[24]

$$V_p^*(z)=V_{iso}^*=V_{iso}^f+\cdot\delta V=V_p^f(z)+\Delta V_p^*(z)+\delta V,$$

with $V_p^f(z)$ and V_{iso}^f average free volumes per molecule in the smectic (with the center of mass at z) and isotropic phases, respectively.

In order to estimate $\Delta V_p^*(z)$ we follow the scheme of our previous work.[24] Let $k(z)$ be the isothermal compressibility of the smectic phase. Then, by definition,

$$k(z)=-\frac{1}{V}\left(\frac{\partial V}{\partial p}\right)_{T,z}, \tag{A6}$$

where V is a small volume around z.

In our previous work we assumed[24] that the compressibility is position independent. In the smectic phase, however, as a result of the density wave along z, $k(z)$ is also a periodic function of z. Since the compressibility-density relation is dominated by a reciprocal dependence, as a rough approximation we assume that the compressibility across the smectic layer is inversely proportional to the density. Since the smectic density wave is weak, we may thus write $k(z)\approx k^0[1-\delta_0\cos(2\pi z/d)]$. Note also that, as a consequence, the amplitude of the compressibility variation across the layer, δ_0 must be directly related to the density wave amplitude; for simplicity we will assume δ_0 to be proportional to $\Lambda(\sigma S+\epsilon\gamma)$.

The average compressibility of the cage surrounding the probe depends on the probe length. We assume that an effective k_z characteristic of the volume around the probe can be taken as the simple average

$$k_z=\int_{z-l/2}^{z+l/2}k(z')dz'/l=k^0+\delta_k\cos(2\pi z/d), \tag{A7}$$

where $\delta_k=-\delta_0\,\mathrm{sinc}(\pi l/d)$. In this manner k_z reduces to $k(z)$ for $l=0$, and takes the average value for $l\geqslant d$.

If Δp_p denotes the associated fluctuation in the pressure leading to increase of the size of the cage by $\Delta V_p^*(z)$, then assuming that the temperature remains constant one can write

$$k_z\simeq-\frac{1}{V_p(z)}\frac{\Delta V_p^*(z)}{\Delta p_p}\bigg|_z. \tag{A8}$$

This should produce a change in the free energy per probe at z

$$\Delta G(z)=V_p(z)\Delta p_p=-\frac{1}{k_z}\Delta V_p^*(z), \tag{A9}$$

provided the ordered phase is otherwise at equilibrium.

On the other hand, since the temperature is constant, the change in the free energy can be associated with the change of the energy of intermolecular interactions averaged over orientations, which in terms of the McMillan mean field approximation can be written as[53]

$$\Delta G(z)=-\frac{U_0}{2}[S\cdot S_p(z)+\Lambda_p(l/d)\sigma\cdot\cos(2\pi z/d)S_p(z)$$

$$+\epsilon_p\Lambda_p(l/d)\gamma\cdot\cos(2\pi z/d)], \tag{A10}$$

where the local orientation parameter of the probe, $S_p(z)$, is given by

$$S_p(z)=\int_0^\pi \sin\theta\,d\theta\,P_2(\cos\theta)\cdot P_\theta(z)$$

with

$$P_\theta(z)=P(\theta,z)/\int_0^\pi \sin\theta\,d\theta\,P(\theta,z).$$

By comparing Eqs. (A9) and (A10) one obtains

$$\Delta V_p^*(z) = \frac{k_z U_0}{2} [\cdot S \cdot S_p(z) + \Lambda_p(l/d)\sigma \cos(2\pi z/d)S_p(z)$$

$$+ \epsilon_p \Lambda_p(l/d)\gamma \cos(2\pi z/d)]; \qquad (A11)$$

whereby the critical free volume $V_p^*(z)$

$$V_p^*(z) = \Delta V_p^*(z) + V_p^f(z) + \delta V \qquad (A12)$$

$$\mathscr{D}(z) = g(V^*)\mathscr{D}^0(T)\exp\left\{ -\frac{\beta_p + \vartheta_p\{SS_p(z) + \Lambda_p(l/d)[\sigma S_p(z) + \epsilon_p\gamma]\cos(2\pi z/d)\}}{T - T_0} \right\}$$

$$\times \exp\left\{ -\frac{\delta_p[SS_p(z)\cos(2\pi z/d) + \Lambda_p(l/d)[\sigma S_p(z) + \epsilon_p\gamma]\cos^2(2\pi z/d)\}}{T - T_0} \right\}, \qquad (A13)$$

where

$$\left. \begin{array}{l} \beta_p = \zeta \cdot \delta V/(\alpha_p \bar{V}_p), \\ \vartheta_p = \zeta \cdot k^0 U_0/(2\alpha_p \bar{V}_p), \\ \delta_p = -\zeta \cdot \delta_0 \, \mathrm{sinc}(l/d) U_0/(2\alpha_p \bar{V}_p). \end{array} \right\} \qquad (A14)$$

It is easy to verify that Eq. (A13) confirms intuitive expectations that diffusion in the hard-core region should be the slowest, while in the aliphatic range, the fastest. In the former case, since $z \approx 0$ (or $\approx d$) and $S_p(z \approx 0) \approx \max$, $\mathscr{D}(z \approx 0)$ will be the smallest, while in the latter case $z \approx d/2$ and $S_p(z \approx d/2) \approx \min$, and the diffusion coefficient becomes the largest.

Equation (A13) forms the basis for considerations of both transverse and longitudinal diffusion. Let us first con-

is finally determined.

The diffusion coefficient in the vicinity of the interlayer position z can now be calculated by substitution of $V_p^*(z)$ into Eq. (A2)

sider transverse diffusion. The probe z position in the layer randomly varies according to the probability function $P(\theta, z)$, such that in the process of diffusion the dependence of the transverse diffusion on z averages out, so the average behavior of the probe is characterized by σ_p, and γ_p, with associated average free energy ΔG given by

$$\Delta G = -\frac{U_0}{2} [S \cdot S_p + \Lambda_p(l/d)\sigma\sigma_p + \epsilon_p\Lambda_p(l/d)\gamma\gamma_p],$$
$$\qquad (A15)$$

and the average compressibility is given by $\langle k \rangle = k^0 + \delta_k\gamma_p$. Therefore, if we assume that the probe diffuses transversely maintaining its average position along the z direction, the (average) transverse diffusion coefficient becomes

$$\mathscr{D}_\perp(T) \approx g_\perp(V^*)\mathscr{D}_\perp^0(T)\exp\left\{ -\frac{\beta_p + \vartheta_0\langle k \rangle [SS_p + \Lambda_p(l/d)\sigma\sigma_p + \epsilon_p\Lambda_p(l/d)\gamma\gamma_p]}{T - T_0} \right\}, \qquad (A16)$$

with $\vartheta_0 = \zeta \cdot U_0/(2\alpha_p \bar{V}_p)$.

It is clear from Eq. (A16) that a probe positioned on average close to the center of the hard core will diffuse transversely much slower than one in the aliphatic region. Note also, that for $\sigma_p \approx 0$ and $\gamma_p \approx 0$, i.e., in the absence of positional order of the probe, we recover the case of the nematic phase.

The case of longitudinal diffusion (i.e., parallel to z) is more complicated since we are dealing with diffusion under the condition of the position-dependent diffusion constant, for which the general form of the diffusion equation is

$$\frac{\partial c}{\partial t} = \frac{\partial}{\partial z}\left[\mathscr{D}(z)\frac{\partial c}{\partial z} + c\frac{\partial U_z}{\partial z} \right], \qquad (A17)$$

where $c(z,t)$ is the spatial distribution of diffusing species, and U_z is an external potential that the diffusing molecule experiences. Two limiting approaches to solving Eq. (A17) are possible. First is one in which the spatial periodicity of

the smectic phase is accounted for utilizing Eq. (A17) as the external potential U_z, with the diffusion coefficient being assumed constant, i.e., $\mathscr{D}(z) = \mathrm{const}$. This type of approach led Moro and Nordio to the macroscopic diffusion coefficient in the form of[35]

$$\mathscr{D}_\parallel = \mathscr{D}_\parallel^0 \left\{ \int_0^d [P_\theta(z)]^{-1} dz \right\}^{-1}, \qquad (A18)$$

where $P_\theta(z)$ is the translational distribution function, and $\mathscr{D}_\parallel^0$ is the position-independent microscopic diffusion constant, cf. Eq. (11).

The other approach is the one that is more natural for our development. We consider diffusion of a particle in the absence of an external potential, $U_z = 0$, but where the diffusion coefficient given by Eq. (A13) is a function of position due to the free-volume effects arising from the $\Delta G(z)$ given by Eq. (A10). Let us consider diffusion of a probe initially at z_0. In the absence of a position-dependent dif-

fusion coefficient, its probability distribution $p(z,t)$ would develop in time according to the Gaussian function

$$p(z,t) = \frac{1}{2(\pi \mathscr{D} t)^{1/2}} \exp[-(z-z_0)^2/(4\mathscr{D} t)] \quad (A19)$$

and the mean square displacement of the probe in t is $\langle (z-z_0)^2 \rangle = 2\mathscr{D} t$. If $\mathscr{D}$ is not constant but rather a periodic function of z as in Eq. (A13), the time dependence of the mean square displacement will reflect this periodicity. However, as diffusion progresses, information about the fine spatial structure of $\mathscr{D}(z)$ will be lost, and the slope of $\langle (z-z_0)^2 \rangle$ vs t converges to $2\mathscr{D}^{\text{macro}}$, the value characteristic for the long-time behavior, i.e., the macroscopic diffusion constant.

We note that this macroscopic diffusion constant can be estimated from the time necessary for the probe to diffuse the distance of the interlayer spacing. The time required for a probe to diffuse over a distance ξ_0, can be considered as a sum of times of residence between small jumps δt (when the free volume expands sufficiently) from one location to another location. The size of the step $\delta \xi$ is always the same since it is defined by the critical free volume V^*, but the time between jumps depends on where the probe is, so one can estimate $\delta t \approx (\delta \xi)^2/2D(\xi)$. Therefore the overall time required for diffusion over the distance ξ_0 is of order of $t = \Sigma \delta t \approx \Sigma (\delta \xi)^2 D^{-1}(z)/2 = \delta \xi \int_0^{\xi_0} D^{-1}(\xi) d\xi/2$. Since $\xi_0/\delta \xi$ is the number of jumps required, the average time between jumps is

$$\delta t^{\text{av}} = \frac{t}{\xi_0/\delta \xi} = \frac{(\delta \xi)^2}{2\xi_0} \int_0^{\xi_0} \frac{d\xi}{D(\xi)}. \quad (A20)$$

Such a definition of the average time is consistent with the definition of the diffusion constant, since for isotropic diffusion Eq. (A20) gives $\delta t^{\text{av}} = (\delta \xi)^2/2D$ as is expected.

In the general case, the average diffusion coefficient is then

$$\mathscr{D}_{\parallel}^{-1}(T) \approx 2\delta t^{\text{av}}/(\delta \xi)^2 = \xi_0^{-1} \int_0^{\xi_0} \mathscr{D}^{-1}(\xi) d\xi. \quad (A21)$$

This result can be alternatively derived through estimation of the average friction coefficient (in units of kT) acting on the diffusing molecule. If Ξ is the friction coefficient, then the resistance to diffusion across a thin film of a fluid of the thickness $\delta \xi$ will be $\Omega_\xi = \Xi \delta \xi$, so the resistance of a layer of the thickness ξ_0 is $\Omega(\xi_0) = \int_0^{\xi_0} \Xi(\xi) d\xi = \xi_0 \Xi^{\text{av}}$, where Ξ^{av} is the average friction coefficient of the layer. Since the friction coefficient is related to the diffusion coefficient via Einstein relation, cf. Eq. (5), by calculating Ξ^{av} one immediately gets Eq. (A21).

In order to evaluate the macroscopic longitudinal diffusion coefficient we set $\xi_0 = d$, i.e., we calculate the average diffusion coefficient over a distance of the interlayer spacing. Substituting Eq. (A13) into Eq. (A21) and for simplicity approximating $S_p(z) \approx S_p^0[1+\delta_S \cos(2\pi z/d)]$, we get

$$\mathscr{D}_{\parallel}^{-1}(T) \approx d^{-1}[g_{\parallel}(V^*)\mathscr{D}_{\parallel}^0(T)]^{-1} \exp[A_0/(T-T_0)]$$

$$\times \int_0^d \exp\{\vartheta_T[A_1 \cos(2\pi z/d)$$

$$+A_2 \cos^2(2\pi z/d) + A_3 \cos^3(2\pi z/d)]\}dz,$$

$$(A22)$$

where $A_0 = \beta_p + k^0 \vartheta_0 SS_p^0$,

$$A_1 = [k^0\delta_S + \delta_k]SS_p^0 + k^0\Lambda_p(l/d)[\sigma S_p^0 + \epsilon_p\gamma],$$

$$A_2 = [k^0\delta_S + \delta_k]\Lambda_p(l/d)\sigma S_p^0 + \delta_k[SS_p^0\delta_S + \epsilon_p\Lambda_p(l/d)\gamma],$$

and

$$A_3 = \delta_k\delta_S\Lambda_p(l/d)\sigma S_p^0,$$

with $\vartheta_T = \vartheta_0/(T-T_0)$.

Note that the form of Eq. (A21) is somewhat similar to the expression obtained by Moro and Nordio, cf. Eq. (A18), although these equations were derived from different initial assumptions.

By substituting $w = 1 - \cos(2\pi z/d)$, Eq. (A22) can be conveniently rewritten as

$$\mathscr{D}_{\parallel}^{-1}(T) \approx \left[4\pi[g_{\parallel}(V^*)\mathscr{D}^0(T)]^{-1} \int_0^2 \exp\{\vartheta_T[-pw+qw^2-A_3w^3]\} \frac{dw}{\sqrt{w}\sqrt{2-w}}\right] \times \exp\left[\frac{A_0+\vartheta_0(A_1+A_2+A_3)}{T-T_0}\right], \quad (A23)$$

where $p = A_1 + 2A_2 + 3A_3$, $q = A_2 + 3A_3$.

The magnitude of the preexponential integral in Eq. (A23) can be estimated if one assumes that the argument of the integrand exponential function is always large, cf. Appendix B, and such the assumption seems justified. For example, experimentally observed values of the activation energy are of the order of several kcal/mol leading to the fact that the argument of the exponential function in Eq. (A22) range from about 10 to about 20 in the relevant temperature range. A similar conclusion can be reached from an estimate of the magnitude of the McMillan potential parameter U_0 which appears in ϑ_0 and ϑ_T. It can be estimated by requiring that the McMillan model fits the observed transition temperatures. Using the McMillan normalization, $U_0 = T_{\text{NI}}/0.2202$,[53] we find for the smectic phase $U_0/(T-T_0) \simeq 4.54T_{\text{NI}}/(T-T_0) \gg 1$.

Applying the result in Eq. (B2) to Eq. (A23) we finally obtain

$$\mathscr{D}_{\parallel}(T) \sim [W(s,\sigma,\gamma|S_p^0)\vartheta_0/(T-T_0)]^{1/2} \times \exp\left\{-\frac{\beta_p + \vartheta_0 k^{\max}\{(1+\delta_S)[S+\Lambda_p(l/d)\sigma] \cdot S_p^0 + \epsilon_p\Lambda_p(l/d) \cdot \gamma\}}{T-T_0}\right\}, \quad (A24)$$

where

$$W(S,\sigma,\gamma\,|\,S_p^0)=\{[\delta_S k^{\max}+(1+\delta_S)\delta_k]S+[(1+2\delta_S)k^{\max}+(1+\delta_S)\delta_k]\Lambda_p(l/d)\sigma\}S_p^0+(k^{\max}+\delta_k)\epsilon_p\Lambda_p(l/d)\gamma,$$
(A25)

and $k^{\max}=k^0+\delta_k\approx k^0-\delta_0\,\mathrm{sinc}(l/d)$.

Since available experimental results suggest that $T\gg T_0$, so $1/(T-T_0)\simeq1/T(1+T_0/T)$ and within experimental error $1/(T-T_0)$ is well approximated by $1/T$ and Eqs. (A16) and (A24) can be simplified to yield

$$\mathscr{D}_\perp(T)\simeq g_\perp(V^*)\mathscr{D}_\perp^0(T)\exp\left\{-\frac{\beta_p+\vartheta_0\langle k\rangle[SS_p+\Lambda_p(l/d)\sigma\sigma_p+\epsilon_p\Lambda_p(l/d)\gamma\gamma_p]}{T}\right\},$$
(A26)

$$\mathscr{D}_\|(T)\simeq g_\|(V^*)\mathscr{D}_\|^0(T)[W(S,\sigma,\gamma\,|\,S_p^0)\vartheta_0/T]^{1/2}\exp\left\{-\frac{\beta_p+\vartheta_0 k^{\max}\{(1+\delta_S)[S+\Lambda_p(l/d)\sigma]\cdot S_p^0+\epsilon_p\Lambda_p(l/d)\cdot\gamma\}}{T}\right\}.$$
(A27)

Equation (A26) together with Eq. (A27) provide the temperature dependence of the principal components of the translational diffusion tensor for a probe of an arbitrary length l diffusing in the smectic phase. Note that a general form of our results is similar to Eqs. (10) and (11) of Moro and Nordio,[35] although with notable differences; a different dependence on temperature of the preexponential factor in Eq. (A27) and explicit dependence of the activation energies on smectic pseudopotential parameters and order parameters.

APPENDIX B

Under the assumption that the argument of the exponential function in the integral

$$J(p,q,A_3)=\int_0^2\exp\{\vartheta_T[-pw+qw^2-A_3w^3]\}\,\frac{dw}{\sqrt{w}\sqrt{2-w}}$$
(B1)

is large, the integral can easily be approximated as follows. First, we note that integration from 1 to 2 will give only a minor contribution to the integral, and, therefore, can be neglected. Second, the integrand has a singularity at $w=0$, which effectively limits the range of significant w's to the vicinity of 0. Therefore we let $1/\sqrt{2-w}\approx1/\sqrt{2}$ and omit the w^2 and w^3 terms in the argument of exponential function, yielding

$$J(p,g,A_3)\simeq\frac{\sqrt{\pi}}{\sqrt{2p}}\,\Phi(\sqrt{p})\approx\frac{\sqrt{\pi}}{\sqrt{2p}},$$
(B2)

since for large p, the error function $\Phi(\sqrt{p})$ is close to unity.

Applying this result to Eq. (A22) one obtains Eq. (A24) for $D_\|$.

[1] T. Svedberg, Kolloid Z. **22**, 68 (1917).
[2] A beautiful review of the Svedberg, Einstein and Smoluchowski work on translational diffusion is given by B. Sredniawa, Theory Preprints, Jagiellonian University, TPJU-6/91, March 1991.
[3] C. K. Yun and A. G. Fredrickson, Mol. Cryst. Liq. Cryst. **12**, 73 (1970).
[4] F. Rondelez, Solid State Commun. **14**, 815 (1974).
[5] G. Heppke, F. Schneider, and A. Sterzl, Z. Naturforsch. Teil A **31**, 1700 (1976).
[6] M.-M. Poo, Annu. Rev. Biophys. Bioeng. **10**, 245 (1981).

[7] G. J. Krüger and H. Spiesecke, Z. Naturforsch. Teil A **28**, 964 (1973).
[8] J. K. Moscicki, Y. K. Shin, and J. H. Freed, in *EPR Imaging and In Vivo EPR*, edited by R. R. Eaton et al. (CRC, Boca Raton, 1991), p. 189.
[9] Y.-K. Shin, U. Ewert, D. E. Budil, and J. H. Freed, Biophys. J. **59**, 950 (1991).
[10] A. J. Leadbetter, F. P. Temme, A. Heidemann, and W. S. Howells, Chem. Phys. Lett. **34**, 363 (1975).
[11] B. Cvikl and U. Dahlborg, Mol. Cryst. Liq. Cryst. **114**, 79 (1984).
[12] C. G. Wade, Annu. Rev. Phys. Chem. **28**, 47 (1977).
[13] A. Nayeem, S. B. Ranavare, V. S. S. Sastry, and J. H. Freed, J. Chem. Phys. **91**, 6887 (1989).
[14] G. J. Krüger, Phys. Rep. **82**, 229 (1982).
[15] M. E. Moseley and A. Loewenstein, Mol. Cryst. Liq. Cryst. **90**, 117 (1982).
[16] M. E. Moseley, J. Phys. Chem. **87**, 18 (1983).
[17] M. E. Moseley and A. Loewenstein, Mol. Cryst. Liq. Cryst. **95**, 51 (1983).
[18] H. Takezoe, M. Hara, S. Ichikawa, and A. Fukuda, Mol. Cryst. Liq. Cryst. **122**, 169 (1985).
[19] G. J. Krüger, H. Spiesecke, R. Van Steenwinkel, and F. Noak, Mol. Cryst. Liq. Cryst. **40**, 103 (1977).
[20] J. P. Hornak, J. K. Moscicki, D. J. Schneider, and J. H. Freed, J. Chem. Phys. **84**, 3387 (1986).
[21] J. K. Moscicki, Y.-K. Shin, and J. H. Freed, J. Magn. Reson. **84**, 554 (1989).
[22] D. A. Cleary, Y. K. Shin, D. J. Schneider, and J. H. Freed, J. Magn. Reson. **79**, 474 (1988).
[23] Y.-K. Shin, and J. H. Freed, Biophys. J. **55**, 537 (1989).
[24] Y.-K. Shin, J. K. Moscicki, and J. H. Freed, Biophys. J. **58**, 445 (1990).
[25] U. Ewert, R. H. Crepeau, C. R. Dunnam, D. Xu, S.-Y. Lee, and J. H. Freed, Chem. Phys. Lett. **184**, 25 (1991); U. Ewert, R. H. Crepeau, S.-Y. Lee, C. R. Dunnam, D. Xu, and J. H. Freed, *ibid.* **184**, 34 (1991).
[26] J. H. Freed, J. Chem. Phys. **66**, 4183 (1977).
[27] W. Lin, and J. H. Freed, J. Phys. Chem. **83**, 379 (1979).
[28] S. A. Zager and J. H. Freed, Chem. Phys. Lett. **109**, 270 (1984).
[29] J. P. Gorcester, S. B. Rananavare, and J. H. Freed, J. Chem. Phys. **90**, 5764 (1989).
[30] A. Nayeem and J. H. Freed, J. Chem. Phys. **93**, 6359 (1989).
[31] J. H. Freed, A. Nayeem, and S. B. Rananavare, in *The Molecular Dynamics of Liquid Crystals*, edited by G. Luckhurst and C. Veracini (Kluwer, Dordrecht, in press).
[32] J. H. Freed, J. Chem. Phys. **96**, 3901 (1992).
[33] A. Nayeem, S. B. Rananavare, V. S. S. Sastry, and J. H. Freed, J. Chem. Phys. **96**, 3912 (1992).
[34] S. B. Rananavare, V. G. K. M. Pisipati, and J. H. Freed, Liq. Cryst. **3**, 957 (1988).
[35] G. Moro and P. L. Nordio, J. Phys. Chem. **89**, 997 (1985).
[36] J. Crank, *The Mathematics of Diffusion* (Clarendon, Oxford, 1976).
[37] R. N. Bracewell, *The Fourier Transform and its Applications* (McGraw-Hill, New York, 1978).
[38] H. Lamb, *Hydrodynamics* (Dover, New York, 1945), Art. 339.

[39] M. Miesowicz, Mol. Cryst. Liq. Cryst. 97, 1 (1983); S. Bhattacharya and S. V. Letcher, Phys. Rev. Lett. 44, 414 (1980).

[40] P. G. de Gennes, The Physics of Liquid Crystals (Oxford University, Oxford, 1974).

[41] G. Vertogen and W. H. de Jeu, Thermotropic Liquid Crystals, Fundamentals (Springer, New York, 1988).

[42] R. P. Shibayeva, L. O. Atovmyan, M. G. Neiganz, L. A. Novakovskaya, and S. L. Ginzburg, Zh. Strukt. Khim. 13, 42 (1972); J. S. Hwang, R. P. Mason, L. P. Hwang, and J. H. Freed, J. Phys. Chem. 79, 489 (1975).

[43] A. J. Leadbetter, J. C. Frost, and J. P. Gaughan, J. Phys. (Paris) 40, 375 (1979).

[44] T. B. Barriott, G. B. Birrell, and O. H. Griffith, J. Am. Chem. Soc. 97, 627 (1975).

[45] L. T. Seidler, and A. J. Hyde, in Advances in Liquid Crystal Research and Applications, edited by L. Bata (Pergamon, Oxford, 1980), p. 561.

[46] J. Janik and J. K. Moscicki, 14 International Liquid Crystal Conference, Pisa, Italy 1992 (to appear in Liq. Cryst.).

[47] K.-S. Chu and D. S. Moroi, J. Phys. Colloq. (Paris) 36, C1-99 (1975).

[48] A. J. Leadbetter in The Molecular Physics of Liquid Crystals, edited by G. R. Luckhurst and G. W. Gray (Academic, New York, 1979).

[49] W. H. de Jeu, Philos. Trans. R. Soc. London Ser. A 309, 217 (1983).

[50] F. Volino and A. J. Dianoux, Mol. Phys. 36, 389 (1978).

[51] G. Moro, P. L. Nordio, and U. Segre, Chem. Phys. Lett. 105, 440 (1984).

[52] G. Moro, U. Segre, and P. L. Nordio, in Nuclear Magnetic Resonance of Liquid Crystals, edited by J. W. Emsley, NATO ASI Ser. C 141 (Reidel, Dordrecht, 1985).

[53] W. L. McMillan, Phys. Rev. 6, 936 (1972).

[54] A. Mircea-Russell, L. Leger, F. Rondelez, and W. H. de Jeu, J. Phys. Colloq. (Paris) 36, C1-93 (1975).

[55] J. Jadzyn and P. Kedziora, Mol. Cryst. Liq. Cryst. 145, 17 (1987).

[56] D. A. Dunmur, 13 International Liquid Crystal Conference, Vancouver, Canada 1990.

[57] See, for example, C. F. Polnaszek, G. V. Bruno, and J. H. Freed, J. Chem. Phys. 58, 3185 (1973).

[58] M. H. Cohen and D. Turnbull, J. Chem. Phys. 31, 1164 (1959).

[59] Z. Pajak, J. Jurga, and K. Jurga, Acta. Phys. Pol. A 40, 893 (1971); T. Podolski, M. Rachwalska, and J. Mayer, Physica B 125, 215 (1984); D. Lewandowska, Acta Phys. Pol. A 67, 539 (1985).

[60] A. C. Diogo and A. F. Martins, J. Phys. (Paris) 43, 779 (1982).